Phase Diagram of the TbBr$_3$-KBr Binary System

L. Rycerz and M. Gaune-Escard[a]

Institute of Inorganic Chemistry and Metallurgy of Rare Elements, Wroclaw University of Technology, Wybrzeze Wyspianskiego 27, 50-370 Wroclaw, Poland
[a] Ecole Polytechnique, Mecanique Energetique, Technopole de Chateau-Gombert, 5 rue Enrico Fermi, 13453 Marseille Cedex 13, France

Reprint requests to M.G.-E.; Fax: +33 (0)4 91 11 74 39;
E-mail: Marcelle.Gaune-Escard@polytech.univ-mrs.fr

The phase equilibrium of the TbBr$_3$-KBr has been established by Differential Scanning Calorimetry. This system has the three compounds K$_3$TbBr$_6$, K$_2$TbBr$_5$, and KTb$_2$Br$_7$ and two eutectics located at ($x_{Tb} = 0.163$ (885 K) and ($x_{Tb} = 0.433$ (697 K). K$_3$TbBr$_6$ undergoes a solid-solid phase transition at 691 K and melts congruently at 983 K with the corresponding enthalpies 8.0 and 48.0 kJ mol^{-1}. K$_2$TbBr$_5$ melts incongruently at 725 K, and KTb$_2$Br$_7$ at 741 K. The latter forms at 694 K, a temperature very close to that (697 K) of one of the two eutectics also existing in the binary system.

Key words: Terbium(III) Bromide; Potassium Bromide; Enthalpy; Phase Diagram; Differential Scanning Calorimetry; Eutectic; Compound; Formation; Decomposition.

1. Introduction

Phase equilibria in lanthanide-alkali halide, LnX$_3$-MX, systems are generally complex, and previous investigations conducted by a variety of techniques [1 – 24] showed that several stoichiometric compounds exist, the stability of which depends both on the nature of cations (Ln, M) and of the halide (X) [25 – 26]. Most studies focussed on the LnCl$_3$-MCl mixtures [27 – 37]. The present work deals with TbBr$_3$-KBr, following the recent phase diagram determination of TbBr$_3$-NaBr [38], and is part of a more general research on the properties of lanthanide(III) bromide – alkali metal bromide systems.

2. Experimental

2.1. Sample Preparation

Terbium bromide, TbBr$_3$, was prepared by sintering bromination of terbium oxide Tb$_4$O$_7$ (Johnson Matthey, 99.9%) with ammonium bromide NH$_4$Br (POCh Gliwice – Poland). The details of this synthesis as well as chemical analysis of the product obtained have been described in [17, 38].

Potassium bromide was Merck Suprapur reagent (min. 99.9%). Prior to use it was progressively heated up to fusion under gaseous HBr atmosphere. HBr in excess was then removed from the melt by argon bubbling.

The mixtures of TbBr$_3$ and KBr (in appropriate proportions) were melted in vacuum-sealed quartz ampoules in an electric furnace. The melts were homogenised by shaking and solidified. These samples were ground in an agate mortar in a glove box. Homogenous mixtures of different composition were used in phase diagram measurements.

All chemicals were handled in an argon glove box with a measured volume fraction of water of about 2×10^{-6} and continuous gas purification by forced recirculation through external molecular sieves.

3. Results

The temperatures and enthalpies of phase transitions of TbBr$_3$-KBr mixtures were measured with a Setaram DSC 121 differential scanning calorimeter. The apparatus and the measurement procedure were described in details in [4 – 6]. Samples (300 – 500 mg) were contained in vacuum-sealed quartz ampoules (about 6 mm diameter, 15 mm length). Enthalpies of transition measurements were conducted at heating and cooling rates between 1 and 5 K min^{-1}. Each experiment was at least done twice on the same sample, and also on dif-

x, TbBr$_3$	T_1 K$_2$TbBr$_5$ transition	T_2 K$_3$TbBr$_6$ transition	T_3 KTb$_2$Br$_7$ formation	T_4 eutectic E$_2$	T_5 K$_2$TbBr$_5$ decomp.	T_6 KTb$_2$Br$_7$ decomp.	T_7 eutectic E$_1$	T_{liquidus} liquidus
0.000	–		–	–	–	–	–	1007
0.050	–	691	–	–	–	–	885	991
0.101	–	691	–	–	–	–	885	955
0.145	–	691	–	–	–	–	885	898
0.182	–	691	–	–	–	–	884	923
0.207	–	691	–	–	–	–	885	943
0.214	–	691	–	–	–	–	884	960
0.247	–	692	–	–	–	–	883	982
0.250	–	691	–	–	–	–	–	983
0.277	661	689	–	–	724	–	–	973
0.294	662	690	–	–	724	–	–	957
0.327	660	689	–	–	724	–	–	927
0.355	658			697	725	–	–	878
0.373	658			696	726	–	–	833
0.397	662			698	727	–	–	762
0.452	661			697	–	–	–	710
0.498	661			697	–	743	–	743
0.529	659		695	695	–	746	–	785
0.531	658		695	697	–	743	–	810
0.554	659			697	–	742	–	803
0.568	657		694	697	–	744	–	838
0.603	662			697	–	741	–	888
0.607	656		694	697	–	744	–	885
0.650	661			696	–	745	–	927
0.658	657		693	697	–	743	–	946
0.680	657		694	–	–	744	–	953
0.699	657		695	–	–	744	–	971
0.739	660		695	–	–	743	–	976
0.758	658		694	–	–	744	–	1003
0.787	656		691	–	–	742	–	1038
0.848	655		688	–	–	740	–	1078
0.9112	653		679	–	–	736	–	1093
0.940	651			–	–	729	–	1100
1.00	–		–	–	–	–	–	1103

Table 1. Results of the DSC experiments with the TbBr$_3$-KBr binary system.

ferent samples of the same composition. The composition of samples used for DSC experiments are given in Table 1.

The DSC investigations were performed on samples with 34 compositions. The corresponding thermograms yielded both the temperature and the fusion enthalpy of the mixtures. The enthalpies of thermal effects obtained from heating and cooling runs were almost the same, the difference not exceeding 2%. However, supercooling was observed on cooling curves, and hence only the heating curves were analysed to gather temperatures and enthalpies.

Figure 1 shows the thermograms obtained for samples with $x = 0.05, 0.250, 0.355$ and 0.607, respectively. In all these heating runs, the highest temperature at which the DSC signal returned to the base line corresponds to the liquidus temperature of each sample.

Figure 2 shows the thermograms obtained for samples with $x = 0.568$ and 0.680: because of particular

features observed during preliminary runs, the same samples were examined during heating rates of 5 and 0.1 K min^{-1}, respectively.

Table 1 gives the temperatures corresponding to the different thermal events and the liquidus temperatures for all these samples.

4. Discussion

The TbBr$_3$-KBr phase diagram was established for the first time in the course of the present work.

In the range $0 < x < 0.250$, where x is mole fraction of TbBr$_3$, three endothermic peaks were present in all heating thermograms (Fig. 1, $x = 0.050$). The first one, at 691 K, is observable in all thermograms up to $x = 0.333$, where it disappears. The second one at 885 K is observed in all samples up to $x = 0.250$, where it disappears. It can be undoubtedly ascribed to the eutectic (E$_1$) effect. The third one at 991 K
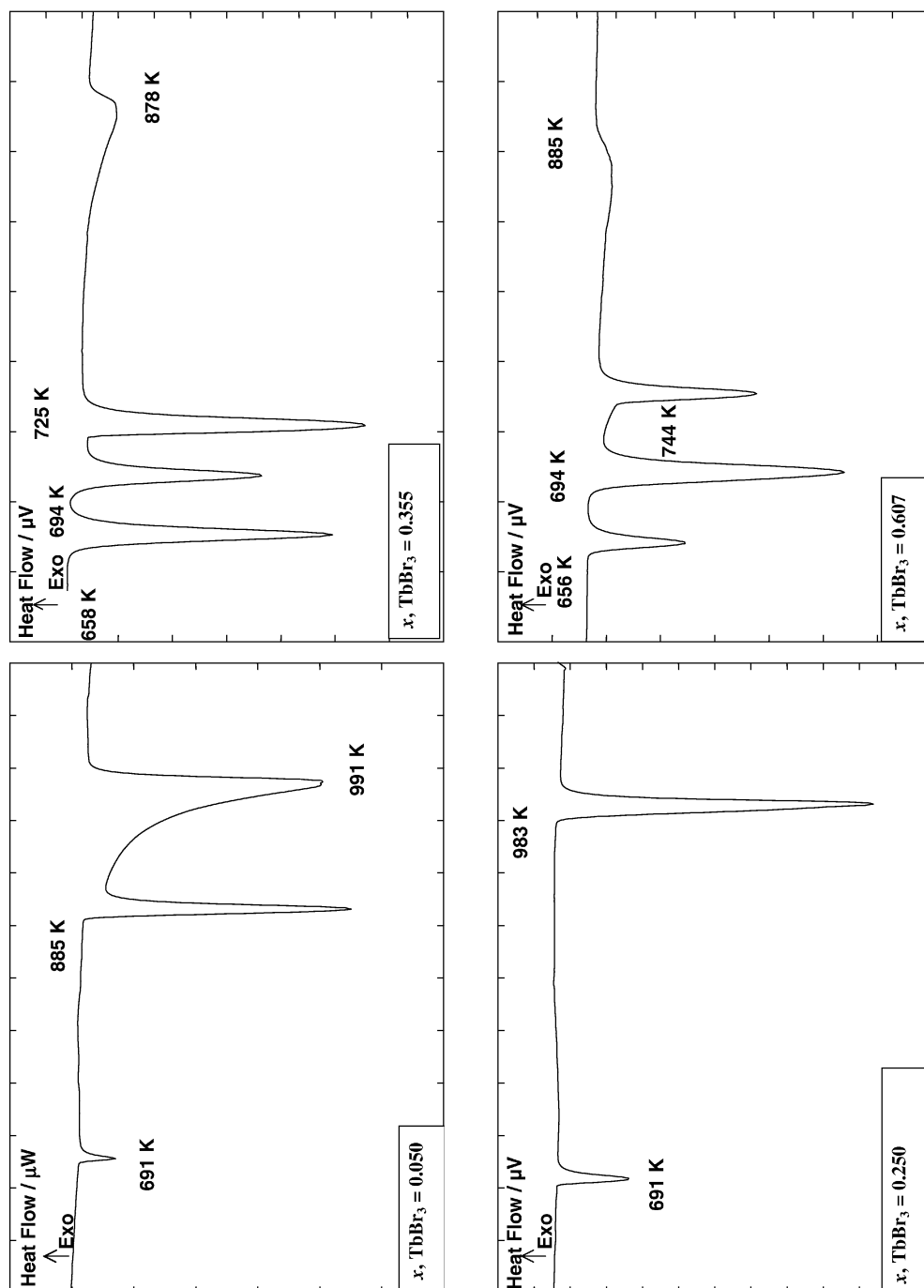
Fig. 1. DSC heating curves for TbBr₃-KBr mixtures, where $x(\text{TbBr}_3) = 0.05$, 0.250, 0.355 and 0.607. The curves show the exothermic heat flow.

corresponds to the liquidus temperature. The eutectic contribution to the enthalpy of fusion was determined and plotted against composition in Figure 3.

This so called Tamman construction makes it possible to evaluate accurately the eutectic composition from the intercept of the two linear parts in Fig. 3, as $x =$
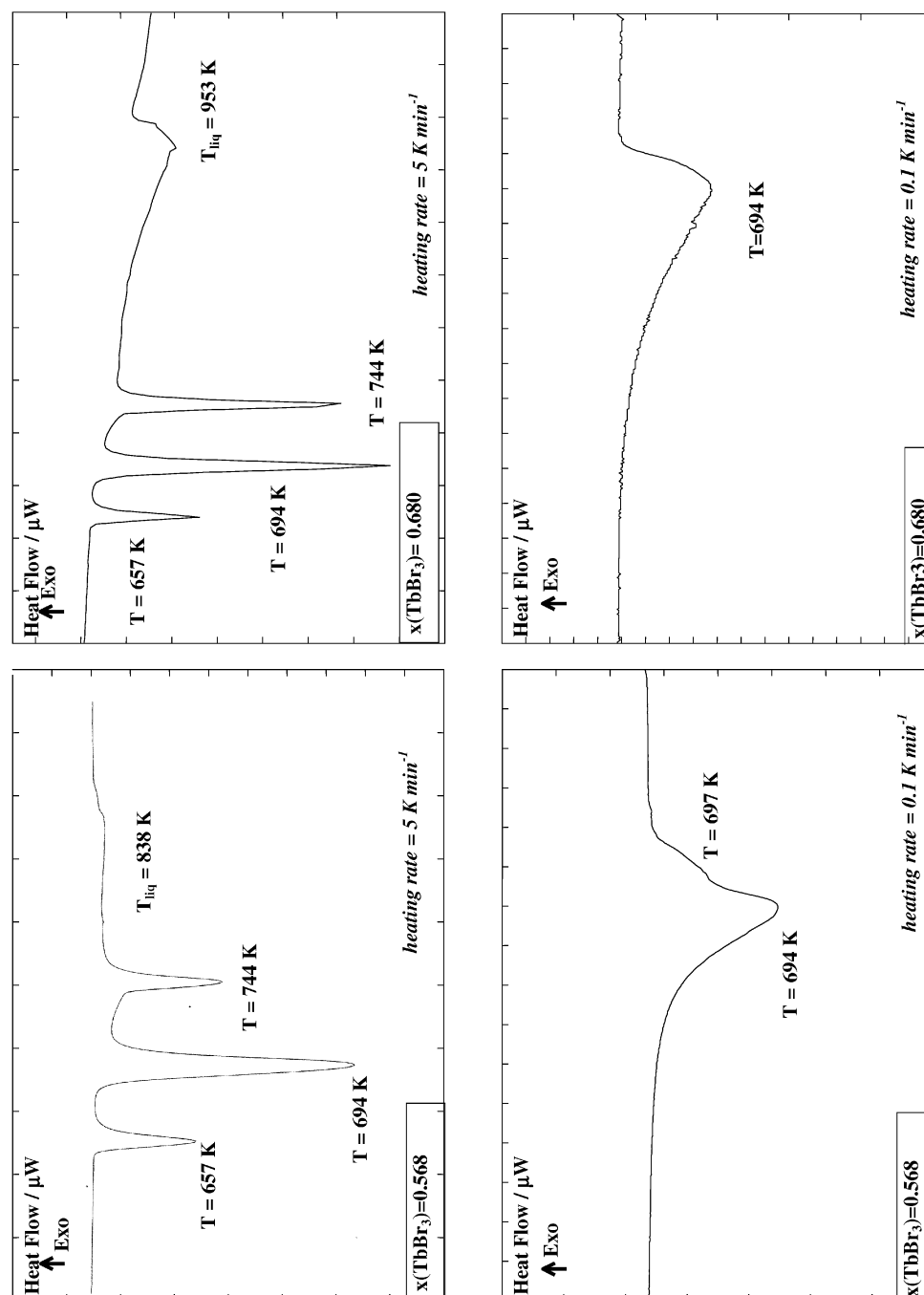
Fig. 2. DSC heating curves with two different heating rates for TbBr$_3$-KBr mixtures, (where x(TbBr$_3$) = 0.568 and 0.680).

0.163. The mixture with eutectic composition melts with an enthalpy, $\Delta_{\text{fus}}H_{\text{m}}$, of about 15.8 kJ mol^{-1}. In this Tamman construction it was assumed that there was no solubility in the solid state. Thus the straight lines intercept the composition axis at $x = 0.0$ and $x = 0.250$.

For the mixture with $x = 0.250$ only two effects were observed on the thermograms (Fig. 1, $x = 0.250$). In
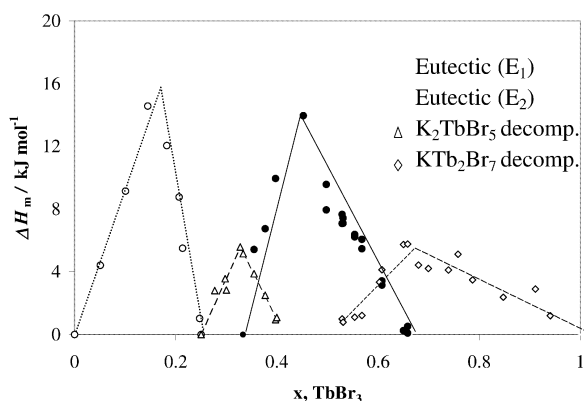
Fig. 3. Determination of eutectic and compound compositions in TbBr$_3$-KBr.
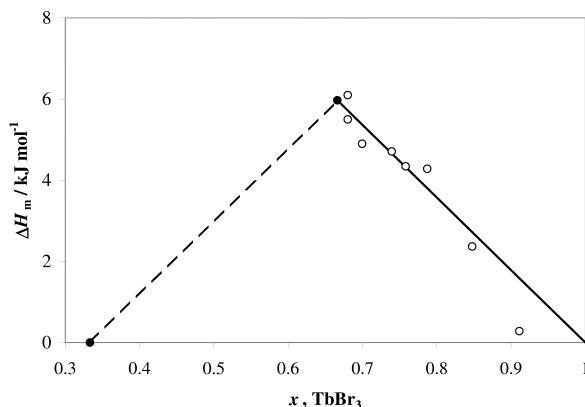

Fig. 4. Graphical evaluation of the thermal effect related to KTb$_2$Br$_7$ formation.
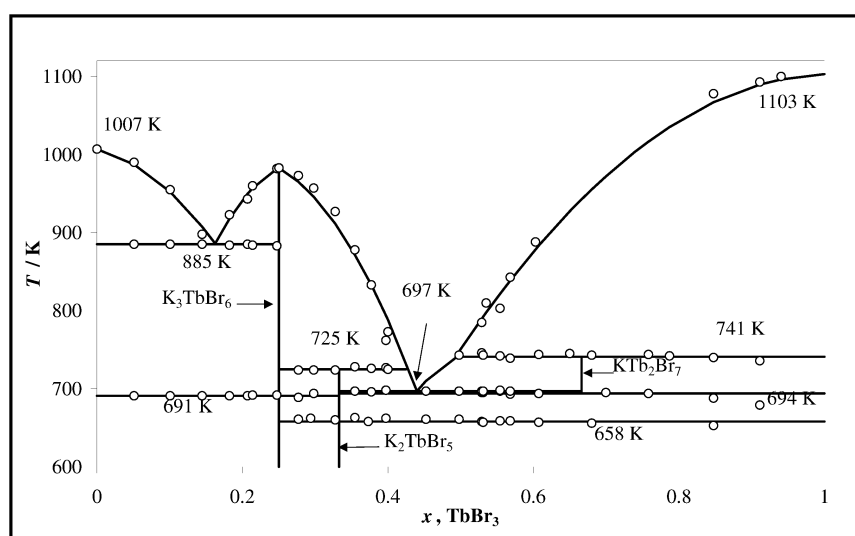

Fig. 5. Phase diagram of TbBr$_3$-KBr.

addition to the effect at 691 K, the peak at 983 K has the typical shape of a congruently melting compound.

From the above observations we deduced that a congruently melting compound exists in the TbBr$_3$-KBr system, which undergoes a solid-solid phase transition at 691 K and melts at 983 K.

The DSC experiments performed at $x > 0.250$, resulted in thermograms with three endothermic peaks, followed by a fourth and final thermal event at the liquidus temperature (Figs. 1, 2). The first and second endothermic effect, at 658 K and 694 K, respectively, is observed in all thermograms. The third peak, also endothermic, is of variable size and occurs either at 725 K, for mixtures with $0.250 < x < 0.420$ (Fig. 1, $x = 0.355$), or at 744 K, for mixtures with higher TbBr$_3$ content (Figs. 1 and 2).

The enthalpy changes corresponding to the effect at 725 K were plotted against composition. From Fig. 3 and the complementary information obtained from the thermograms it was concluded that the phase diagram contains also the compound K$_2$TbBr$_5$. The composition of this characteristic point was determined from Fig. 3 as $x = 0.328$, a value in excellent agreement with the theoretical value 0.333 for K$_2$TbBr$_5$.

The thermograms for the x-range $0.330 - 1.0$ indicated that another compound may exist in this range, and if so, the thermal event observed repeatedly at 741 K would correspond to its decomposition. The enthalpies of the effect observed at 741 K in mixtures with x higher than 0.498 were plotted against x in Fig. 3: this plot includes two linear parts that intercept at $x = 0.665$. This composition is consistent with
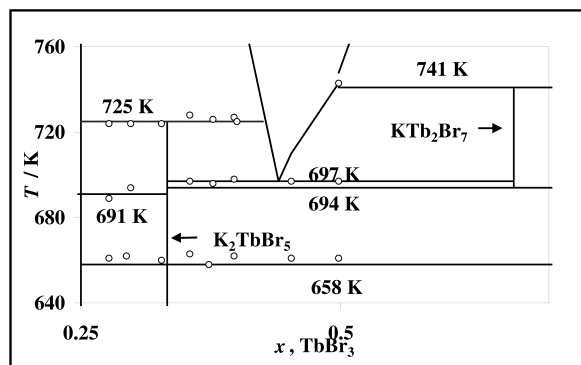
Fig. 6. Details of the TbBr$_3$-KBr phase diagram around the eutectic E$_2$.

the existence of KTb$_2$Br$_7$. Thus, the thermal effect at 741 K can be ascribed to the incongruent melting of KTb$_2$Br$_7$.

It is very likely that this compound forms at 694 K, a temperature very close to the eutectic E$_2$ temperature (697 K). Therefore in addition to the experimental runs at the rate 5 K min^{-1}, the same samples were processed at the very low rate 0.1 K min^{-1} as indicated in Figure 2. They clearly indicate that for samples of composition $0.666 < x < 1.0$, the peak observed at 694 K is a single one, while that observed in samples of composition $0.333 < x < 0.666$ results from the superimposition of two effects, at 694 K and 697 K, respectively.

However, even at extremely low heating rates it was impossible to separate these close effects shown in the thermogram in Fig. 2 ($x = 0.568$). Therefore a different procedure was used in order to evaluate both the compositions at which they occur and the corresponding enthalpy changes. Since the effect at 694 K, for $x \geq 0.666$, corresponds to KTb$_2$Br$_7$ formation, the related enthalpy was plotted against composition in Figure 4. The straight, line obtained from the least-squares fitting of the experimental results, indicated a linear variation, from which the enthalpy related to the effect of KTb$_2$Br$_7$ formation (black circle in Fig. 4) was deduced at the *ad hoc* composition. It was assumed that

the enthalpy related to the formation of this compound, at compositions less than $x = 0.666$, is also a linear function of composition and that its limiting value at $x = 0.333$, is $\Delta H_m = 0$ kJ mol^{-1}. This straight line, drawn from these two enthalpy values (at $x = 0.333$ and $x = 0.666$) for the KTb$_2$Br$_7$ compound is marked as a dashed line in Figure 4. The enthalpy values related to effect of KTb$_2$Br$_7$ formation obtained in this way make it possible to separate the eutectic contribution E$_2$ from the global effect (formation of the compound at 694 K and the eutectic at 697 K). The result obtained graphically is plotted against concentration in Figure 3. The eutectic composition ($x = 0.433$) was determined from the intercept of the two linear parts in Figure 3. The fusion enthalpy of the eutectic mixture is $\Delta_{\text{fus}}H_m = 13.8$ kJ mol^{-1}.

The complete phase diagram of the TbBr$_3$–KBr binary system is presented in Figure 5. The details of the system around the eutectic E$_2$ are presented in Figure 6.

5. Conclusion

The TbBr$_3$-KBr binary system is characterised by the eutectics E$_1$ and E$_2$, located at $x = 0.163$; 885 K and $x = 0.433$; 697 K, respectively, and the three compounds K$_3$TbBr$_6$, K$_2$TbBr$_5$, and KTb$_2$Br$_7$.

K$_3$TbBr$_6$ undergoes a solid-solid phase transition at 691 K and melts congruently at 983 K, with the corresponding enthalpies 8.0 and 48.0 kJ mol^{-1}.

K$_2$TbBr$_5$ melts incongruently at 725 K and KTb$_2$Br$_7$ at 741 K. The latter forms at 694 K, a temperature very close to that of the eutectic E$_2$ (697 K).

[1] M. Gaune-Escard, L. Rycerz, W. Szczepaniak, and A. Bogacz, J. Alloys Comp. **204**, 193 (1994).
[2] M. Gaune-Escard, L. Rycerz, W. Szczepaniak, and A. Bogacz, J. Alloys Comp. **204**, 189 (1994).
[3] M. Gaune-Escard, A. Bogacz, L. Rycerz, and W. Szczepaniak, Thermochim. Acta **236**, 59 (1994).

[4] M. Gaune-Escard, A. Bogacz, L. Rycerz, and W. Szczepaniak, Thermochim. Acta **236**, 67 (1994).
[5] M. Gaune-Escard, L. Rycerz, and A. Bogacz, J. Alloys Comp. **204**, 185 (1994).
[6] R. Takagi, L. Rycerz, and M. Gaune-Escard, Denki Kagaku **62,3**, 240 (1994).

[7] M. Gaune-Escard, L. Rycerz, W. Szczepaniak, and A. Bogacz, Thermochim. Acta **236**, 51 (1994).

[8] M. Gaune-Escard, L. Rycerz, W. Szczepaniak, and A. Bogacz, Thermochim. Acta **279**, 1 (1996).

[9] M. Gaune-Escard, L. Rycerz, W. Szczepaniak, and A. Bogacz, Thermochim. Acta **279**, 11 (1996).

[10] M. Gaune-Escard, L. Rycerz, and R. Takagi, J. Alloys Comp. **257**, 134 (1997).

[11] M. Gaune-Escard and L. Rycerz, Molten Salt Forum, **5 – 6**, 217 (1998).

[12] M. Gaune-Escard and L. Rycerz, Z. Naturforsch. **54a**, 229 (1999).

[13] L. Rycerz and M. Gaune-Escard, Z. Naturforsch. **54a**, 397 (1999).

[14] L. Rycerz and M. Gaune-Escard, The International George Papatheodorou Symposium, Patras, September 17 – 18, 1999, Proceedings, p. 95 – 99.

[15] F. Da Silva, L. Rycerz, and M. Gaune-Escard, Z. Naturforsch. **56a**, 647 (2001).

[16] F. Da Silva, L. Rycerz, and M. Gaune-Escard, Z. Naturforsch. **56a**, 653 (2001).

[17] L. Rycerz and M. Gaune-Escard, Z. Naturforsch. **56a**, 859 (2001).

[18] P. Gaune, M. Gaune-Escard, L. Rycerz, and A. Bogacz, J. Alloys Comp. **235**, 143 (1996).

[19] K. Fukushima, T. Ikumi, J. Mochinaga, R. Takagi, M. Gaune-Escard, and Y. Iwadate, J. Alloys Comp. **260**, 75 (1997).

[20] A. K. Adya, R. Takagi, and M. Gaune-Escard, Z. Naturforsch. **53a**, 1037 (1998).

[21] R. Takagi, F. Hutchinson, P. A. Madden, A. K. Adya, and M. Gaune-Escard, J. Phys. Condensed Matter **11**, 64 (1999).

[22] M. P. Tosi, Molten Salts From Fundamentals to Applications, M. Gaune-Escard ed., Kluwer Academic Publishers, 2002, p. I.

[23] F. Da Silva and M. Gaune-Escard, Advances in Molten Salts: From Structural Aspects to Waste Processing, M. Gaune-Escard (ed.) Begell House Inc. 125 (1999).

[24] M. Sakurai, R. Takagi, A. A. Adya, and M. Gaune-Escard, Z. Naturforsch. **53a**, 655 (1998).

[25] H. J. Seifert, J. Therm. Anal. Cal. **7**, 789 (2002).

[26] L. Rycerz, High Temperature Characterization of LnX$_3$ and LnX$_3$-AX Solid and Liquid Systems (Ln=Lanthanide, A=Alkali, X=Halide): Thermodynamics and Electrical Conductivity, Ph.D. Thesis, Marseille 2003.

[27] H. J. Seifert, H. Fink, and G. Thiel, J. Less-Common Metals **110**, 139 (1985).

[28] H. J. Seifert, J. Sandrock, and G. Thiel, J. Therm. Anal. **31**, 1309 (1986).

[29] H. J. Seifert, J. Sandrock, and J. Uebach, Z. Anorg. Allg. Chem. **555**, 143 (1987).

[30] H. J. Seifert, H. Fink, and J. Uebach, J. Therm. Anal. **33**, 625 (1988).

[31] G. Thiel and H. J. Seifert, Thermochim. Acta **133**, 275 (1988).

[32] H. J. Seifert and J. Sandrock, Z. Anorg. Allg. Chem. **587**, 110 (1990).

[33] H. J. Seifert, J. Sandrock, and G. Thiel, Z. Anorg. Allg. Chem. **598/599**, 307 (1991).

[34] H. J. Seifert, H. Fink, and B. Baumgartner, J. Solid State Chem. **107**, 19 (1993).

[35] S. Mitra and H. J. Seifert, J. Solid State Chem. **115**, 484 (1995).

[36] M. Roffe and H. J. Seifert, J. Alloys Comp. **257**, 128 (1997).

[37] Ch. Zheng and H. J. Seifert, J. Solid State Chem. **135**, 127 (1998).

[38] L. Rycerz, M. Cieslak-Golonka, E. Ingier-Stocka, and M. Gaune-Escard, J. Therm. Anal. Cal. **72**, 231 (2003).